Int. J. Heat Mass Transfer. Vol. 36, No. 15, pp. 3743–3749, 1993
Printed in Great Britain

0017–9310/93 $6.00 + 0.00

Oscillatory thermocapillary flow in a rectangular cavity

JYH-CHEN CHEN and FARN-SHIUN HWU
Department of Mechanical Engineering, National Central University, Chung-Li, Taiwan 32054, R.O.C.

(*Received* 20 *July* 1992 *and in final form* 5 *March* 1993)

Abstract—In this study, thermocapillary convection in a two-dimensional rectangular cavity with an upper, deformable free surface has been studied numerically. A wide range of values of the Marangoni number, *Ma*, is considered for the low Prandtl number fluid ($Pr = 0.01$) with the aspect ratio (A = height/length) fixed to be 0.5. The present computational results show that the thermocapillary flow may undergo an oscillatory motion when the Marangoni number is larger than a certain critical value, with a frequency of oscillation. If the Marangoni number is less than this critical value, the steady thermocapillary convection is obtained. The critical Marangoni number for the appearance of the oscillatory flow increases as the capillary number decreases and the Biot number increases.

1. INTRODUCTION

THERMOCAPILLARY convection is a fluid motion induced by surface tension gradients on a liquid–gas interface arising from temperature gradients. It plays an important role in many technological and engineering science applications such as laser surface melting, crystal growth from melt, migration of a droplet or a gas bubble, or coating, etc. The influence of thermocapillary convection becomes significant for small-scale systems or low-gravity environments.

Experiments on thermocapillary convection in liquid bridges performed by Preisser *et al.* [1], Kamotani *et al.* [2], and Velten *et al.* [3] have shown that a steady thermocapillary flow may change into an oscillatory flow when a dimensionless parameter known as the Marangoni number exceeds a particular critical value, and the other parameters are kept fixed. Understanding of the nature of this change is still limited. Smith and Davis [4, 5] conducted a linear stability analysis of thermocapillary flow in a shallow cavity. They considered separately two flow instabilities: convective instability due to thermocapillary convection effect, and surface-wave instability caused by surface deformation. In their predictions, the surface-wave instability is dominant for systems with low Prandtl numbers. Carpenter and Homsy [6] employed a linear theory to investigate the instability of steady thermocapillary flow in a square cavity and found that the flow is stable up to Marangoni numbers several times larger than critical values experimentally observed in the bridges. In their analyses, the influences of surface deformation and three-dimensional disturbances are not taken into account. Hadid and Roux [7] computed the thermocapillary flow in long horizontal cavities with a flat interface for fluids with low Prandtl numbers. For the Marangoni numbers they considered, the oscillatory flow was not predicted. As mentioned by Ostrach *et al.* [8] and Chen *et al.* [9] the oscillatory flow may be established through the effect of a liquid–gas interface deformation. Kazarinoff and Wilkowski [10] have performed numerical calculations for a two-dimensional unsteady thermocapillary flow in an axially symmetric liquid bridge, taking into account surface deformation. Their results showed that the flow may bifurcate from a steady state to unsteady motions. One may suspect that the oscillation of thermocapillary flow is a consequence of a complex coupling between the interface deformation and thermocapillary convection.

In the present study, the thermocapillary convection in a rectangular cavity with surface deformation is investigated using a series of numerical computations. The numerical technique for integrating the time-dependent, nonlinear Navier–Stokes and energy equations is a modified version of that used by Chen *et al.* [11]. In this scheme, a finite-difference method combined with a time-dependent boundary-fitted curvilinear coordinate system has been used. Our purpose is to attempt to demonstrate that the steady thermocapillary flow may begin to oscillate due to the influence of the free-surface deformation. The effects of Marangoni, capillary, and Biot numbers on the flow pattern are examined for the low Prandtl number fluid ($Pr = 0.01$) with the aspect ratio (height/length) fixed at 0.5.

2. MATHEMATICAL FORMULATION

The physical configuration consists of a rectangular cavity of length L and height H, as shown in Fig. 1. It contains an incompressible Newtonian fluid of density ρ, dynamic viscosity μ, kinematic viscosity ν, specific heat c_p, and thermal diffusivity α. The iso-

NOMENCLATURE

A	aspect ratio
Bi	Biot number
Ca	capillary number
c_p	specific heat
h	location of the free surface
H	height of cavity
h_g	surface heat transfer coefficient
L	length of the cavity
Ma	Marangoni number
p	dimensionless pressure
Pr	Prandtl number
Re	Reynolds number
t	dimensionless time
T	temperature
T_c	temperature at $x' = L$
T_h	temperature at $x' = 0$
u	dimensionless horizontal velocity
v	dimensionless vertical velocity
V	dimensionless volume of the liquid
x	dimensionless horizontal coordinate
x'	horizontal coordinate
y	dimensionless vertical coordinate
y'	vertical coordinate.

Greek symbols

α	thermal diffusivity
γ	surface-tension temperature coefficient
Θ	dimensionless temperature
μ	dynamic viscosity
ν	kinematic viscosity
ρ	density
σ	surface tension
σ_0	mean value of free surface
ψ	stream function
ω	vorticity.

Subscripts

x, y	derivative with respect to x, y.

thermal rigid side walls at $x' = 0$ and $x' = L$ are differentially heated and are maintained at different fixed temperatures T_h and T_c, respectively. The bottom rigid wall is thermally insulated, and the free surface is bounded by a passive gas of negligible density and viscosity with temperature distribution $f(x) = T_c + (T_h - T_c)x'/L$. The surface tension is considered as a linear function of temperature

$$\sigma(T) = \sigma_m - \gamma[T - (T_h + T_c)/2] \quad (1)$$

where σ_m is the mean value of the surface tension and γ is the rate of decrease of surface tension with temperature.

We chose the scales for length, velocity, time, and pressure to be H, $\gamma(T_h - T_c)/\mu$, $\mu H/\gamma(T_h - T_c)$, and $\gamma(T_h - T_c)/H$, respectively. The dimensionless temperature is defined by

$$\Theta = \frac{T - T_c}{T_h - T_c}.$$

By eliminating the pressure, the resulting dimensionless governing equations for the unsteady two-dimensional motion of the liquid are

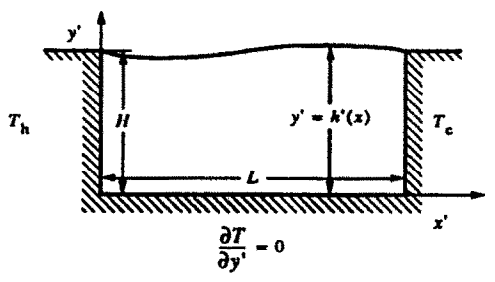

FIG. 1. Schematic diagram of the physical system.

$$Re(\omega_t + u\omega_x + v\omega_y) = (\omega_{xx} + \omega_{yy}) \quad (2a)$$

$$Ma(\Theta_t + u\Theta_x + v\Theta_y) = (\Theta_{xx} + \Theta_{yy}) \quad (2b)$$

$$-\omega = \psi_{xx} + \psi_{yy}. \quad (2c)$$

Here, the steam function ψ and vorticity ω are defined by

$$u = \psi_y$$

$$v = -\psi_x$$

$$\omega = v_x - u_y.$$

The two dimensionless parameters which appear are the Reynolds and Marangoni numbers, given by

$$Re = \frac{\gamma(T_h - T_c)H}{\mu\nu}$$

and

$$Ma = \frac{\gamma(T_h - T_c)H}{\mu\alpha}$$

respectively. The Prandtl number is obtained from the quotient Ma/Re. The boundary conditions are

$$\psi = 0, \quad \omega = -\psi_{xx}, \quad \Theta = 1; \quad x = 0 \quad (3a\text{–}c)$$

$$\psi = 0, \quad \omega = -\psi_{xx}, \quad \Theta = 0; \quad x = 1/A \quad (4a\text{–}c)$$

$$\psi = 0, \quad \omega = -\psi_{yy}, \quad \Theta_y = 0; \quad y = 0 \quad (5a\text{–}c)$$

$$-\psi_x = \psi_y h_x + h_t$$

$$-p + 2(1+h_x^2)^{-1}[h_x(\psi_{xx} + h_x\psi_{xy}) - (\psi_{xy} + h_x\psi_{yy})]$$
$$= Ca^{-1}h_{xx}(1+h_x^2)^{-3/2}(1 - Ca\,\Theta)$$

$$(1-h_x^2)\omega = (1+h_x^2)^{1/2}(\Theta_x + h_x\Theta_y)$$
$$-4h_x\psi_{xy} - 2\psi_{xx}(1-h_x^2)$$

$$(\Theta_y - \Theta_x h_x) =$$
$$-Bi(1+h_x^2)^{1/2}[\Theta - 1/2 + Ax]; \quad y = h(t,x). \quad (6a\text{–}d)$$

Equations (3)–(5) express the kinematic, no-slip, and thermal conditions, whereas (6a) is the kinematic condition on the free surface. Equations (6b, c) represent the shear and normal-stress balances at the free surface, respectively. The dimensional parameters appearing in boundary conditions are the capillary number, the Biot number and the aspect ratio, given by

$$Ca = \frac{\gamma(T_h - T_c)}{\sigma_0}$$

$$Bi = h_g H/k$$

and

$$A = H/L$$

respectively, where h_g is the surface heat transfer coefficient.

The liquid volume remains constant for any instant

$$\int_0^{1/A} h(t,x)\,dx = V \tag{7}$$

where V is the dimensionless volume. To complete the problem, the type of contact by the free-surface at the solid wall must be specified. The contact conditions assume that the liquid sticks to the solid end walls

$$h(t,0) = 1, \quad h(t,1/A) = 1. \tag{8}$$

Equations (2)–(8) form the so-called unsteady thermocapillary free boundary problem, where the location of the free surface is not known a priori, but is part of the overall solution. As the solutions of the previous time step are known, an instant solution of the velocity and temperature field can be determined from equation (2) and boundary conditions (3)–(6) by assigning a specific shape to the interface and discarding the normal-stress condition (6b). The normal-stress balance is used to check whether the interface shape is a proper solution. When the normal-stress balance cannot be satisfied, a new interface is selected to reduce the error.

3. NUMERICAL PROCEDURE

The numerical technique used previously by Chen *et al.* [11] to study unsteady thermocapillary convection in a rectangular cavity has been used to solve a system (2) with appropriate conditions. The finite-difference code is a generalization of the steady algorithm developed by Chen *et al.* [12]. The code uses a time-dependent, boundary-fitted curvilinear coordinate system [13], having coordinate lines coincident with the surface boundary at any instant. In this approach, the time-dependent physical domain, because of the variation of interface, is always mapped onto the square computational domain which is fixed in time and space. Grid-stretching transformations have been employed to provide good resolution near the gas–liquid interface. The grid point locations in the computational domain are time-independent, but the corresponding points in the physical domain are time-dependent, because of the shape of the interface as a function of time. The stream-function equation is solved by the line-successive-overrelaxation (LSOR) method, while the vorticity and temperature equations are solved by the semi-implicit predictor–corrector-multiple-iteration (PCMI) technique. All spatial derivatives at the interior points are discretized using central-difference formulas with second-order accuracy, and time derivatives are approximated using a three-point backward difference with second-order accuracy. A brief summary of our computational procedure is as follows:

(1) The steady-state solution for the particular values of Bi, Ca, A, Ma and Pr is selected as the initial state, and at $t > 0$, Ma is suddenly changed to the desired value.

(2) Initial guesses for ψ, ω, Θ, and h at the beginning of a new time step are extrapolated from the values of the two previous time steps (with modification of the first time step).

(3) The boundary-fitted curvilinear coordinate system has been generated numerically.

(4) The PCMI method is used to integrate the differential equations for ω and Θ.

(5) The ψ equation is solved iteratively using the LSOR method. The iteration process is assumed to converge when the relative error of two successive iterations is less than 10^{-7}.

(6) Steps (4)–(5) are repeated until the relative error of two successive iterations for ω and Θ is less than 10^{-7}.

(7) Check the normal-stress condition, and if it is not satisfactory, modify the interface shape to reduce the difference between the normal stress and the surface tension (see details in ref. [10]).

(8) Return to step (3) and repeat iteratively until all equations and boundary conditions are satisfied to a predetermined level of accuracy.

(9) Return to step (2) for the next time step.

4. RESULTS AND DISCUSSION

The numerical calculations were made in double-precision arithmetic on the National Central University IBM 540 and HP 9000/730 workstations. Computations were performed for the cases in which the aspect ratio is 0.5 and the Prandtl number is 0.01. The range of Marangoni numbers considered here is from 1 to 250. The time step used for the calculations was $\Delta t = 0.4$, and there were a total of 81 spatial mesh points in the x-direction and 61 in the y-direction. Test computations showed these to be sufficiently small to ensure accuracy and convergence. When the density of spatial mesh points was inadequate, the irregular streamline patterns were found near the cold wall for higher Ma. Based on the results of Chen *et al.* [12], this can be expected since the largest velocity gradient

exists near the cold wall for $Pr < 1$. For $Ca = 0.01$ and $Bi = 0$, the difference in the critical Marangoni numbers calculated using grids of 81×61 and 51×41 is not very significant. For $Ma = 15$, the streamline pattern and the interface shape for 51×41 grid points are irregular near the cold wall. On the contrary, the results for 81×61 do not show this behaviour.

Our computation results show that the steady thermocapillary flows could be obtained only for Marangoni numbers below a certain critical value, Ma_c, that depends on capillary and Biot numbers. When $Ma > Ma_c$, the oscillatory flow is predicted. Figure 2 shows the time history of the maximum height, h_{max}, of the free surface for $Ca = 0.01$ and $Bi = 0$ with four different Ma. For $Ma < Ma_c$ ($Ma_c = 2.15$), the maximum height of the free surface oscillates and decays with time before it reaches equilibrium. As $Ma > Ma_c$, the gas–liquid interface, the flow field, and the temperature field begin to oscillate for a fixed period after the initial transient period. From Fig. 2, it is obvious that the magnitude of free-surface deflection for the oscillating flow is amplified as Ma increases. The whole gas–liquid interface is oscillating like a standing wave. Figure 3 illustrates the interface shape for $Ma = 10$, $Ca = 0.01$ and $Bi = 0$ at three different times from a complete period. The maximum amplitude of the interface is at $t = 351.2$, and $t = 342.4$ is the minimum. The locations of the maximum and minimum heights of the interface always appear at the same positions in the x-coordinate.

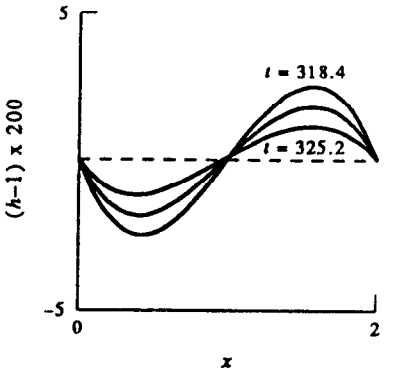

FIG. 3. The surface deflection for $Ma = 10$, $Ca = 0.01$ and $Bi = 0$ at three different times comprising a complete period.

The time history of the maximum value of the stream function within the cavity, ψ_{max}, and the temperature at the maximum height of interface, T_{hmax}, for $Ma = 10$, $Ca = 0.01$ and $Bi = 0$ are illustrated in Fig. 4. From Fig. 2(c) and Fig. 4, we see that after the initial time period, the flow and temperature fields oscillate with the same period as the interface shape. Kamotani *et al.* [2] conjectured that the time-lag behaviour between the interface flow and the return flow near the bottom wall is the reason for the appearance of an oscillatory motion. The time lag only appears in the unsteady thermocapillary flow with a surface deformation [11]. To demonstrate the time-lag behaviour of the oscillatory flow, the variation of h_{max}, ψ_{max}, and T_{hmax} for a complete period is illustrated in Fig. 5. The present results show that time

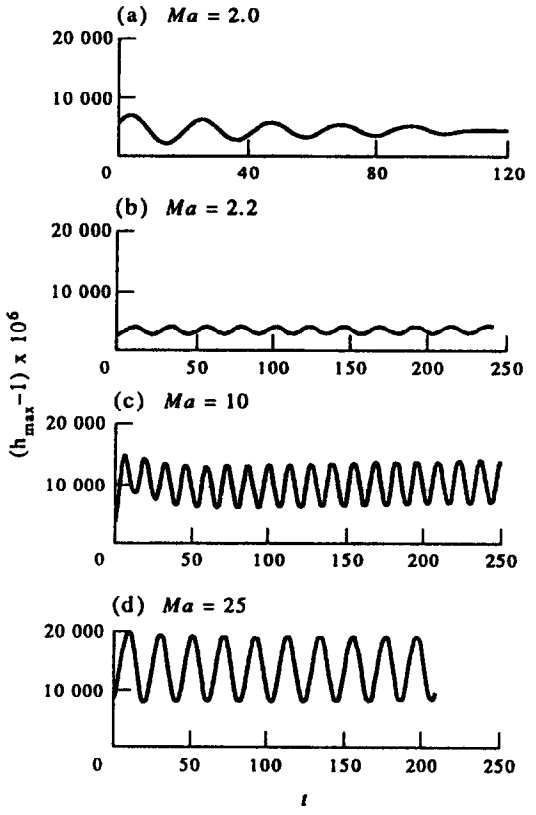

FIG. 2. The time history of h_{max} for $Ca = 0.01$ and $Bi = 0$ with four different Ma.

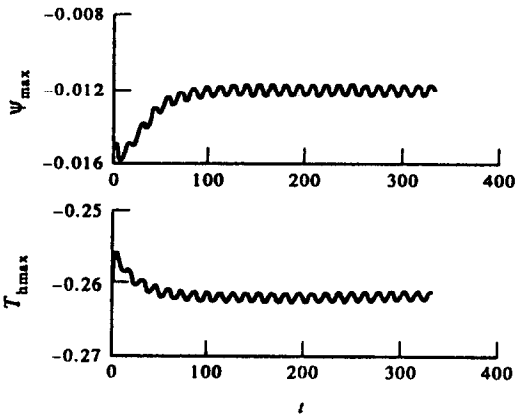

FIG. 4. The time history of ψ_{max} and T_{hmax} for $Ma = 10$, $Ca = 0.01$ and $Bi = 0$.

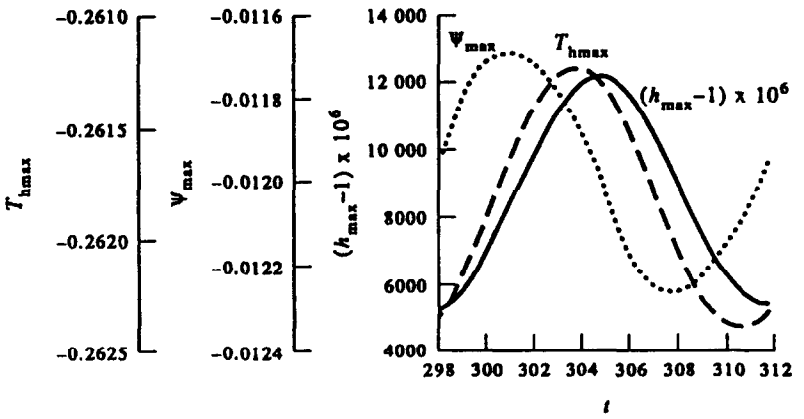

FIG. 5. The variation of H_{max}, ψ_{max}, and T_{hmax} for $Ma = 10$, $Ca = 0.01$ and $Bi = 0$ for a complete period.

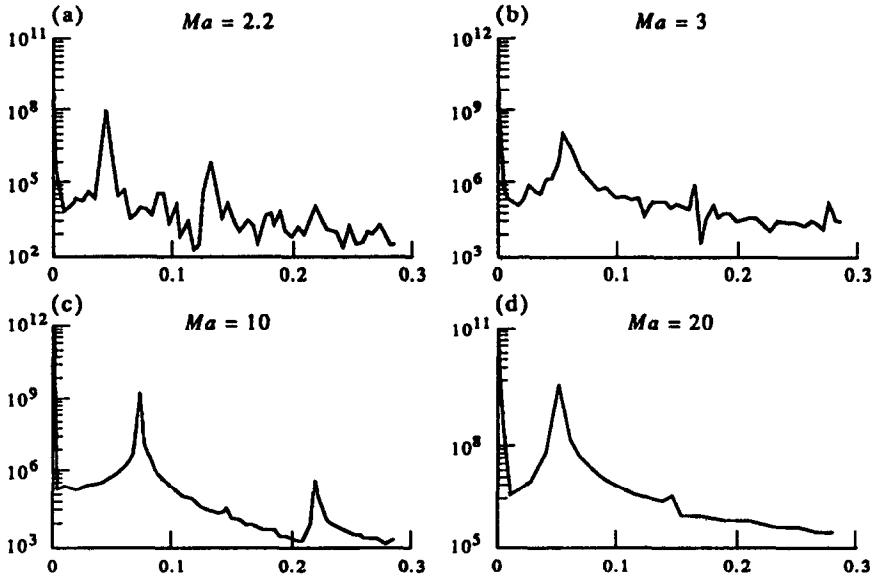

FIG. 6. The frequency-spectra plot for $Ca = 0.01$ and $Bi = 0$ with four different Ma.

lags exist between h_{max}, ψ_{max}, and T_{hmax}. It is obvious that the time-lag between the interface flow and the return flow occurs in the present system for $Ma > Ma_c$. Similar behaviours also are predicted by Chen *et al.* [11] and Lai [14] who studied the unsteady thermocapillary motion caused by periodic time-dependent heating along the interface.

The frequency-spectra plot for the h_{max} is given in Fig. 6. For $Ma = 2.2$ just above Ma_c, the main frequency is $f_0 = 0.042$ with minor frequencies of $f_k = (2k+1)f_0$. The noise signals for $Ma < 10$ are possibly generated by the truncation and round-off errors. The influence of the noise signal on the frequency-spectra plot decreases as Ma increases. Figure 7 shows the relationship between the main frequency and Marangoni number for $Ca = 0.01$ and $Bi = 0$.

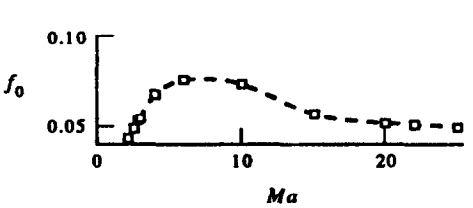

FIG. 7. The main frequency vs Marangoni number for $Ca = 0.01$ and $Bi = 0$.

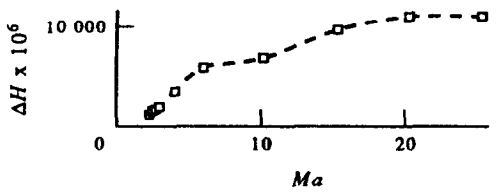

FIG. 8. The oscillatory amplitude vs Marangoni number for $Ca = 0.01$ and $Bi = 0$.

The main frequency for $Ma_c < Ma < 6$ increases with increasing Ma, until it reaches a maximum value around $Ma = 6$. The main frequency for $Ma > 6$ decays slowly and approaches a constant with increasing Ma. Figure 8 demonstrates the effect of the Marangoni number on the oscillatory amplitude, ΔH, at the location of the maximum height. For $Ma_c < Ma < 6$, the oscillatory amplitude increases linearly as Ma increases. When $Ma > 6$, the oscillatory amplitude starts to increase slowly, and then approaches a constant as Ma continues to increase. We define the oscillatory speed, C, as the ratio of the oscillatory amplitude to the half period of the oscillatory. From Fig. 9, we can see that the oscillatory speed increases exponentially and then approaches a constant value when Ma increases.

The influence of the capillary number, which governs the degree of the surface deformation, on the critical Marangoni number is shown in Fig. 10 for $Bi = 0$. In this figure, we can see that the thermocapillary flow is destabilized by the surface deformation. The linear-theory results for zero aspect ratio [5] also show similar trends. The critical Marangoni number predicted by the present computations increases exponentially as the capillary number decreases. From this figure, we can conjecture that for $Ca = 0$ the oscillatory flow may not occur, or that the oscillatory thermocapillary flow will appear for much higher Marangoni numbers. The oscillatory flow for the zero capillary number could not also be predicted in the earlier linear-stability analyses of Carpenter and Homsy [6]. The linear-theory results for the zero aspect ratio [4, 5] showed that for small Prandtl number fluids, the interaction of the surface deformation and underlying bulk shear flow are major reasons for the instability of the thermocapillary flow. It is obvious that the surface deformation is an important factor in causing the oscillation of the thermocapillary flow. The critical Marangoni number predicted by Smith and Davis [5] is $Ma_c = 1.9$ for $Pr = 0.01$, $Ca = 0.0001$, and $Bi = 0$. Our computational results show that the critical Marangoni number is $Ma_c = 15.9$ which is much higher than that predicted by Smith and Davis. But this can be expected since the flow may be stabilized by the viscosity effect due to the presence of the side wall. The effect of the order of the Biot numbers is also of interest. Figure 11 is a plot of Ma_c vs Bi for $Ca = 0.0001$. Obviously, the steady thermocapillary flow is stabilized by the heat transfer at the interface. The critical Marangoni number increases as the Biot number increases.

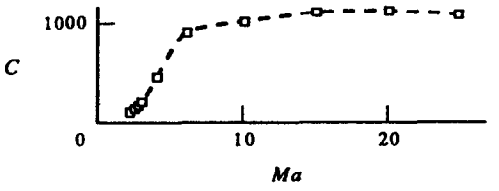

FIG. 9. The oscillatory speed vs Marangoni number for $Ca = 0.01$ and $Bi = 0$.

5. CONCLUSIONS

Steady thermocapillary flows could not be obtained, and the oscillatory flows are predicted when the Marangoni number exceeds a certain critical value. When the Marangoni number is less than this critical value, the thermocapillary flow approaches a steady-state solution after initial transient behaviour. Time-lag behaviours between the velocity field, surface temperature variation, and surface deformation

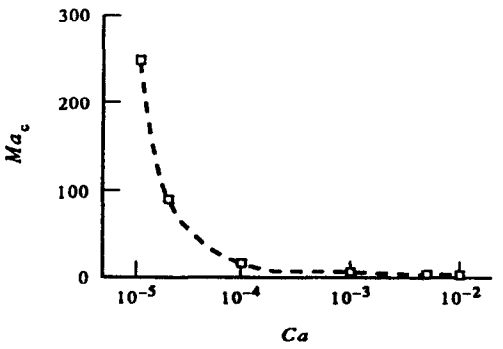

FIG. 10. The capillary number vs critical Marangoni number for $Bi = 0$.

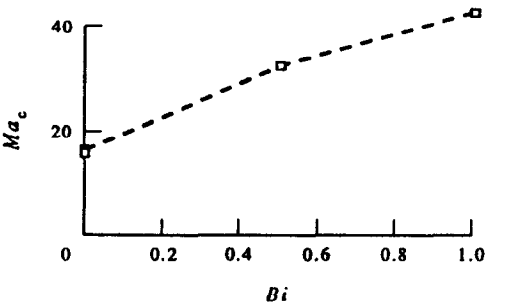

FIG. 11. The Biot number vs critical Marangoni number for $Ca = 0.0001$.

predicted by Chen *et al.* [11] and Lai [14] have also been observed in the present oscillatory flows. The oscillatory speed of the flows increases as the Marangoni number increases. With further increases in the Marangoni number, the oscillatory speed almost approaches a constant value. The value of Ma_c is strongly dependent on the degree of surface deformation and the heat convection between the interface and the ambient. The present computational results are consistent with the results of Smith and Davis [5] in that the critical Marangoni number decreases as the capillary number increases.

In the present analysis, the three-dimensional effect is not included and the contact condition at triple phase is restricted to the case in which the liquid sticks to the end walls. The motion of the interface for the present oscillatory flow is like a standing wave. The travelling-wave phenomenon is predicted by the linear-theory results for the zero aspect ratio [5]. This phenomenon may be obtained using the present code, as long as the contact angle is fixed at the liquid–solid–gas tri-junction. Of course, this must be verified by further computations which are currently underway.

Acknowledgement—This work was supported by the National Science Council of the Republic of China under Grant No. NSC 82-0401-E-008-092.

REFERENCES

1. F. Preisser, P. Schwabe and A. Scharmann, Steady and oscillatory thermocapillary convection in liquid columns with free cylindrical surface, *J. Fluid Mech.* **126,** 545–567 (1983).
2. Y. Kamotani, S. Ostrach and M. Vargas, Oscillatory thermocapillary convection in a simulated floating-zone configuration, *J. Crystal Growth* **66,** 83–90 (1984).
3. R. Velten, R. Schwabe and A. Scharmann, The periodic instability of thermocapillary convection in cylindrical liquid bridges, *Physics Fluids A* **3,** 267–279 (1991).
4. M. K. Smith and S. H. Davis, Instabilities of dynamic thermocapillary liquid layers Part 1. Convective instabilities, *J. Fluid Mech.* **132,** 119–144 (1983).
5. M. K. Smith and S. H. Davis, Instabilities of dynamic thermocapillary liquid layers: Part 2. Surface wave instabilities, *J. Fluid Mech.* **132,** 145–162 (1983).
6. B. M. Carpenter and G. M. Homsy, High Marangoni number convection in a square cavity: Part II, *Physics Fluids A* **2,** 137–149 (1990).
7. H. B. Hadid and B. Roux, Thermocapillary convection in long horizontal layers of low-Prandtl-number melts subject to a horizontal temperature gradient, *J. Fluid Mech.* **221,** 77–103 (1990).
8. S. Ostrach, Y. Kamotani and C. L. Lai, Oscillatory thermocapillary flows, *PCH PhysicoChem. Hydrodyn.* **6,** 585–599 (1985).
9. J. C. Chen, J. C. Sheu and Y. T. Lee, Maximum stable length of nonisothermal liquid bridges, *Physics Fluid A* **2,** 1118–1123 (1990).
10. N. D. Kazarinoff and J. S. Wilkowski, Bifurcations of numerical simulated thermocapillary flows in axially symmetric float zones, *Physics Fluid A* **2,** 1797–1807 (1990).
11. J. C. Chen, W. C. Chen and F. S. Hwu, Numerical computations of unsteady thermocapillary convection in a rectangular cavity with surface deformation, *Heat Transfer in Metals and Containerless Processing and Manufacturing*, HTD **162,** 89–95 (1991).
12. J. C. Chen, J. C. Sheu and S. S. Jwu, Numerical computation of thermocapillary convection in a rectangular cavity, *Numer. Heat Transfer A* **17,** 287–308 (1990).
13. J. F. Thompson, Z. U. A. Warsi and C. W. Masin, *Numerical Grid Generation*. North-Holland, Amsterdam (1985).
14. C. L. Lai, Unsteady thermocapillary flows and free surface oscillations in reduced gravity environments, *Acta Astronautica* **22,** 171–181 (1990).